

## Zn<sub>0.9</sub>Co<sub>0.1</sub>O-based diluted magnetic semiconducting thin films

S. Ramachandran,<sup>a)</sup> Ashutosh Tiwari, and J. Narayan

NSF Center for Advanced Materials and Smart Structures, Department of Materials Science & Engineering, North Carolina State University, Raleigh, North Carolina 27695-7916

(Received 8 December 2003; accepted 28 April 2004; published online 10 June 2004)

Here we report a systematic study of structural, optical, and magnetic measurements on epitaxial Zn<sub>0.9</sub>Co<sub>0.1</sub>O films grown on *c*-plane sapphire single crystal, at various temperatures (500–650 °C), using pulsed-laser deposition. The main emphasis in this work has been on the correlation of microstructure with properties, specifically with magnetic properties and the fate of cobalt ions into substitutional sites versus precipitates. The reasons for room-temperature ferromagnetism are explored, and convincingly proved to be one of the inherent properties of the material. Most importantly, the presence of nanoclusters of any magnetic phase was ruled out. This was determined by high-resolution transmission electron microscopy, coupled with electron energy loss spectroscopy and STEM-Z (scanning transmission electron microscopy-atomic number) contrast studies. © 2004 American Institute of Physics. [DOI: 10.1063/1.1764936]

Recent advances in the emerging technologies of spintronics and related devices have attracted widespread attention. Consequently, the quest for integrating the semiconducting properties with the magnetic properties in a material has become a prerequisite for successful fabrication of useful devices such as high-performance read-heads, nonvolatile memories, and other state of the art storage devices.<sup>1,2</sup> Diluted magnetic semiconductors (DMS), obtained by incorporating magnetic impurities into host semiconductors, serve just this purpose. There have been many advances in the recent past in this area, particularly the wide band gap, III–V and II–VI based DMS materials, where not only the charge but also the spin of the electron is used to bring about the unique functionalities.<sup>3</sup> Until now, applications using such materials were possible only at low temperatures owing to the low  $T_c$  of such DMS,<sup>4</sup> though theoretical predictions of Dietl *et al.*<sup>5</sup> and Kazunori *et al.*<sup>6</sup> have suggested the possibility of room-temperature ferromagnetism in such materials. In particular, zinc oxide based thin films doped with some transition metal elements (e.g., Co) have already strengthened this belief by exhibiting a  $T_c$  much above 300 K.<sup>3</sup> Ueda *et al.* found that a few Co doped ZnO films showed systematic ferromagnetic behavior and the rest of the doped films showed spin glass behavior.<sup>7</sup> Although, room temperature (RT) ferromagnetism was ruled out in Mn, Cr, or Ni<sup>8</sup> doped film a recent report<sup>9</sup> has found it otherwise in Mn doped ZnO. However, because of the lack of detailed microstructural characterization in these works, there is still a lot of controversy over the fate of these magnetic impurities (nanosize clusters/precipitates and/or individual atoms in substitutional sites) and whether the magnetic behavior is an intrinsic property of the films or due to the presence of nanoclusters of a magnetic phase or a combination of both.<sup>10</sup> For example, a recent study<sup>11</sup> reported the presence of Co nanoclusters in Co<sup>+</sup> implanted ZnO (exhibiting RT ferromagnetism), but did not preclude the possibility of the component of the magnetic property due to Co substitution of the Zn in ZnO lattice.

In this work, we report the properties of Zn<sub>0.9</sub>Co<sub>0.1</sub>O with special emphasis on clarifying the origin of magnetic

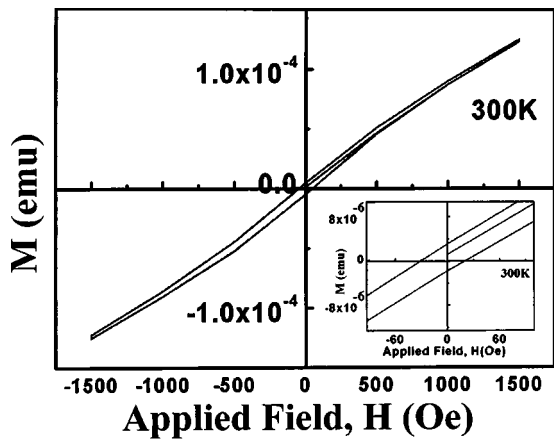
behavior from the perspective of the microstructural characteristics, specifically the presence of nanoclusters. We have probed into this aspect to provide direct evidence for the cause of ferromagnetism using various techniques including high resolution transmission electron microscopy and EELS.

Zn<sub>0.9</sub>Co<sub>0.1</sub>O thin films were grown on the *c* plane of sapphire single crystal substrates, by pulsed-laser deposition.<sup>12</sup> The target used was prepared by the conventional solid state reaction technique. A pulsed KrF excimer laser with a wavelength of 248 nm was used for the deposition. The energy density and the repetition rate of the laser beam were 2–3 J/cm<sup>2</sup> and 10 Hz, respectively. Thin film growth was carried out in the temperature range of 500–650 °C and at a pressure of 10<sup>-6</sup> Torr, for 15–20 min yielding films of about 0.5 μm thickness. X-ray diffraction of the grown films was carried out using a Rigaku x-ray diffractometer with Cu Kα radiation and Ni Filter. Magnetic measurements were performed using a Quantum Design (superconducting quantum interference device) magnetometer in the temperature range of 10–300. Structural characterization was done using a JEOL-2010 field-emission transmission electron microscope equipped with GIF (Gatan Image Filter) tuning attachment. Optical measurements (absorption/transmission) were made using a Hitachi Spectrophotometer.

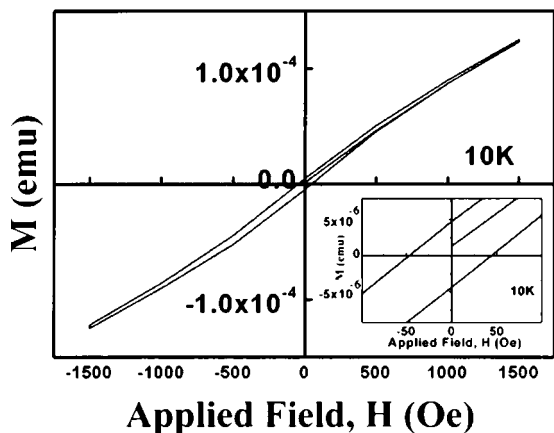
Results from magnetic characterization, for the sample grown at 500 °C are shown in Fig. 1.  $M$  versus  $H$  at 300 K and 10 K and the corresponding insets indicated a coercivity of the thin film to be around 35 and 50 Oe, respectively.  $M$  versus  $T$  conducted at a field of 500 G shows an almost linear drop in the moment (of ~3% over the entire temperature range with a relation  $M = -4 \times 10^{-9} \times T + 3 \times 10^{-5}$ ) with increasing temperature. Similar behavior has been reported in earlier works as well.<sup>3</sup>

X-ray diffraction suggests the formation of a highly aligned phase in this temperature range, with a *c*-axis preferred orientation, as shown in Fig. 2(a). Comparison of (0002) peak of Zn<sub>0.9</sub>Co<sub>0.1</sub>O with the corresponding peak of pure ZnO [see the inset of Fig. 2(a)] suggests an increase in the lattice parameter. This increase in “*c*” as a function of Co concentration is consistent with substitution of Zn by Co.<sup>7</sup> In addition, very slow scans near the peaks of both hexagonal

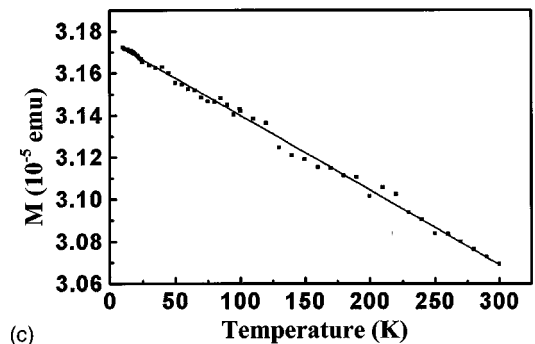
<sup>a)</sup>Electronic mail: sramach@unity.ncsu.edu



(a)



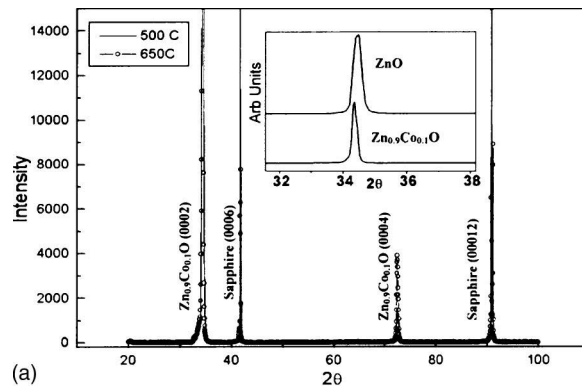
(b)



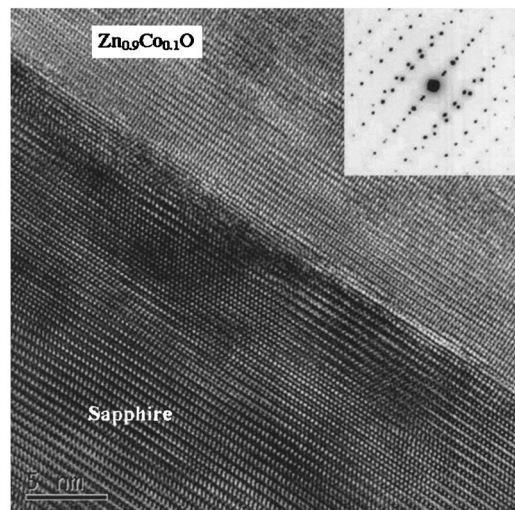
(c)

FIG. 1. (a)  $M$  vs  $H$  of  $Zn_{0.9}Co_{0.1}O$  thin film at room temperature; (b)  $M$  vs  $H$  of  $Zn_{0.9}Co_{0.1}O$  thin film at 10 K; (c)  $M$  vs  $T$  of the  $Zn_{0.9}Co_{0.1}O$  thin film over the temperature range 10–300 K. Insets of (a) and (b) show the magnified portion of the plot near origin.

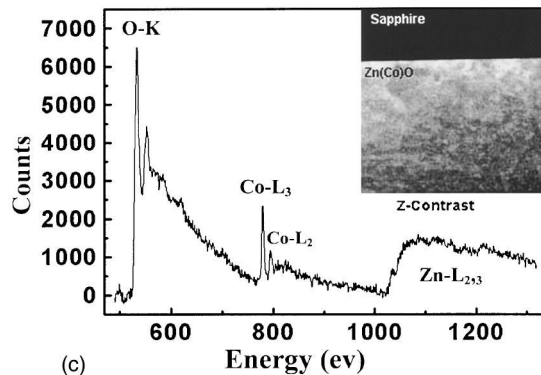
and cubic cobalt phases showed no signatures of any kind of additional phases in our thin films. Detailed high-resolution TEM and Z-contrast studies were conducted to investigate the different phases that might have formed in the nanosize range and to determine the fate of Co atoms which could not be detected by x-ray analysis. This aspect is very important to analyze the origin of magnetic properties of such systems. Figure 2(b) shows the high-resolution micrograph of the thin film. The inset shows a perfect epitaxy of the film with the substrate, having the following orientation relationships:  $(0002)_s \parallel (0002)_f$ ,  $(01\bar{1}0)_s \parallel (\bar{2}110)_f$ ,  $(2\bar{1}\bar{1}0)_s \parallel (01\bar{1}0)_f$ . Diffraction contrast bright field images did not show any possibility of clustering or nanosized particles, because any precipitates or clusters of that order of size should show up as a



(a)



(b)



(c)

FIG. 2. (a) X-ray diffraction of the  $Zn_{0.9}Co_{0.1}O$  films grown at 500 and 650°C. Inset: Change in lattice parameter compared to pure zinc oxide; (b) high resolution image of the interface. Inset: Diffraction pattern of the interface; (c) background reduced electron energy loss spectrum from the bulk of the film. Inset: STEM Z-Contrast image.

black–white contrast images with the black–white vector always perpendicular to the  $\mathbf{g}$  vector in the case of three-dimensional precipitates, or making a certain angle for two-dimensional precipitates.<sup>13</sup>

Further characterization was done using electron energy loss spectroscopy (EELS) to determine the oxidation state at various points in the film. EELS spectra were obtained from three different points, viz. near a dislocation, near the interface, and inside the film. The peaks do not shift with different points of observation, indicating that the oxidation state of cobalt does not change at various points in the film. Figure 2(c) shows the spectrum from the bulk of the film. The characteristic cobalt  $L_2$  and  $L_3$  peaks can be seen. Further calcu-

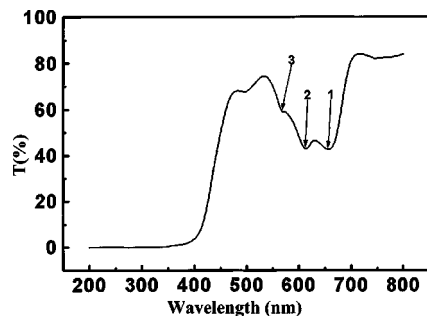


FIG. 3. Optical transmission spectrum of  $\text{Zn}_{0.9}\text{Co}_{0.1}\text{O}$  film grown at  $500^\circ\text{C}$ .

lations on the ratio of the integrated intensity counts, done on the  $L_3$  and  $L_2$  peaks of cobalt, correspond to an oxidation state of +2. This strengthens the belief that Co substitutes Zn in the lattice uniformly. In addition, STEM-Z contrast imaging was done which also did not show the presence of any precipitates as is evident from the inset in Fig. 2(c). Similar results were obtained from samples grown at higher temperatures of  $650^\circ\text{C}$ .

Figure 3 shows optical absorption and transmission measurements on the sample grown at  $500^\circ\text{C}$ . The spectrum shows characteristic absorption edges around 658, 616, and 568 nm wavelengths, which are labeled as (1), (2), and (3), respectively. In the literature,<sup>14,15</sup> these edges are correlated with the  $d-d$  transitions of the tetrahedrally co-ordinated  $\text{Co}^{2+}$  ions and attributed, respectively, to the  ${}^4A_2(F) \rightarrow {}^2E(G)$ ,  ${}^4A_2(F) \rightarrow {}^4T_1(P)$ , and  ${}^4A_2(F) \rightarrow {}^2A_1(G)$ . This indicates that the Co ions have substituted the  $\text{Zn}^{2+}$  ions. This shows the presence of cobalt in a tetrahedral crystal field in the +2 state supporting the results from the structural characterization as well.

Having ruled out the possibility of the presence of nanoclusters through our structural and optical investigations, we infer that the presence of nanoclusters could not be the cause of the observed room-temperature ferromagnetism. Furthermore, if the nanoclusters were of such small size that they could not be detected by HRTEM, then they should exhibit superparamagnetic behavior with a much lower Blocking temperature,<sup>16</sup> which was not the case. These facts help to rule out the possibility of the presence of nanoclusters/precipitates as the cause of magnetic behavior. Hence we conclude that the room-temperature ferromagnetism is an inherent property of the material caused by the presence of cobalt in high-spin configuration in a tetrahedral crystal field. High spin state of  $\text{Co}^{2+}$  (3/2 moments per ion) arises because of the crystal field splitting of  $3d$  state in  $t_{2g}$  and  $e_g$  orbitals, with four electrons in  $e_g$  state and three unpaired electrons in  $t_{2g}$  state.

In conclusion, we have doped  $\text{Co}^{2+}$  ions in ZnO to produce  $\text{Zn}_{0.9}\text{Co}_{0.1}\text{O}$  thin films grown by pulsed-laser deposition on  $c$ -plane sapphire single crystal substrates. The films were single crystalline, epitaxially grown on sapphire with a  $30^\circ$  or  $90^\circ$  rotation relative to the substrate. These films exhibited ferromagnetism at room temperature. Atomic scale structural characterization including high resolution TEM, STEM-Z contrast, and EELS was done to provide evidence for the absence of any nano-sized clusters or second phase. Optical measurements also showed the presence of the cobalt ions in a tetrahedral crystal field. This proves that the magnetic properties of the film were a result of the replacement of  $\text{Zn}^{2+}$  in the ZnO lattice by  $\text{Co}^{2+}$  ions. This is possible because of the capabilities to exceed the constraints posed by thermal equilibrium,<sup>17</sup> with the help of pulsed-laser deposition. Further work in the area could be to determine the maximum concentration that can be doped into ZnO and to study the effect on the structural as well as magnetic properties.

This work was partly supported by ARO and NSF. The authors want to thank J. Prater, G. Duscher, and A. Kvit for discussions in TEM analysis and J. Bousquet for help in magnetic measurements.

- <sup>1</sup>G. A. Prinz, *Science* **282**, 1660 (1998).
- <sup>2</sup>S. A. Wolf, D. D. Awschalom, R. A. Buhrman, J. M. Daughton, S. von Molnár, M. L. Roukes, A. Y. Chtchelkanova, and D. M. Treger, *Science* **294**, 1488 (2001).
- <sup>3</sup>S. Y. Yang, A. B. Pakhomov, S. T. Hund, and C. Y. Wong, *IEEE Trans. Magn.* **38**, 2877 (2002).
- <sup>4</sup>T. Dietl, *Nat. Mater.* **2**, 646 (2003).
- <sup>5</sup>T. Dietl, H. Ohno, F. Matsukura, J. Cibert, and D. Ferrand, *Science* **287**, 1019 (2000).
- <sup>6</sup>K. Sato and H. K. Yoshida, *Mater. Res. Soc. Symp. Proc.* **666**, F4.6.1 (2001).
- <sup>7</sup>K. Ueda, H. Tabata, and T. Kawai, *Appl. Phys. Lett.* **79**, 988 (2001).
- <sup>8</sup>A. Tiwari, C. Jin, A. Kvit, D. Kumar, J. F. Muth, and J. Narayan, *Solid State Commun.* **121**, 371 (2002).
- <sup>9</sup>P. Sharma, A. Gupta, K. V. Rao, F. J. Owens, R. Sharma, R. Ahuja, J. M. Osorio Guillen, B. Johansson, and G. A. Gehring, *Nat. Mater.* **2**, 673 (2003).
- <sup>10</sup>S. J. Pearton, C. R. Abernathy, M. E. Overberg, G. T. Thaler, D. P. Norton, N. Theodoropoulou, A. F. Hebard, Y. D. Park, F. Ren, J. Kim, and L. A. Boatner, *J. Appl. Phys.* **93**, 1 (2003).
- <sup>11</sup>D. P. Norton, M. E. Overberg, S. J. Pearton, K. Pruessner, J. D. Budai, L. A. Boatner, M. F. Chisholm, J. S. Lee, Z. G. Khim, Y. D. Park, and R. G. Wilson, *Appl. Phys. Lett.* **83**, 5488 (2003).
- <sup>12</sup>D. B. Chrisey and G. H. Hubler, *Pulsed Laser Deposition of Thin Films* (Wiley, New York, 1994).
- <sup>13</sup>P. Hirsch, A. Howie, R. B. Nicholoso, D. W. Pashley, and M. J. Whelan, *Electron Microscopy of Thin Crystals*, 2nd ed. (Kreiger, Malbar, FL, 1977), p.317.
- <sup>14</sup>P. Koidl, *Phys. Rev. B* **15**, 2493 (1977).
- <sup>15</sup>K. J. Kim and Y. R. Park, *Appl. Phys. Lett.* **81**, 1420 (2002).
- <sup>16</sup>M. Klimenkov, J. von Borany, W. Matz, D. Eckert, M. Wolf, and K. H. Müller, *Appl. Phys. A: Mater. Sci. Process.* **74**, 571 (2002).
- <sup>17</sup>T. Dietl and H. Ohno, *MRS Bull.* **28**, 714 (2003).